



## **$\beta$ -Cyclodextrin-NHC-Gold(I) Complex ( $\beta$ -ICyD)AuCl: A Chiral Nanoreactor for Enantioselective and Substrate-Selective Alkoxy cyclization Reactions**

Coralie Tugny, Natalia Del Rio, Mehdi Koohgard, Nicolas Vanthuyne, Denis Lesage, Kajetan Bijouard, Pinglu Zhang, Jorge Meijide Suárez, Sylvain Roland, Etienne Derat, et al.

### **► To cite this version:**

Coralie Tugny, Natalia Del Rio, Mehdi Koohgard, Nicolas Vanthuyne, Denis Lesage, et al..  $\beta$ -Cyclodextrin-NHC-Gold(I) Complex ( $\beta$ -ICyD)AuCl: A Chiral Nanoreactor for Enantioselective and Substrate-Selective Alkoxy cyclization Reactions. ACS Catalysis, 2020, 10 (11), pp.5964–5972. 10.1021/acscatal.0c00127 . hal-02885939

**HAL Id: hal-02885939**

**<https://hal.science/hal-02885939>**

Submitted on 23 Mar 2021

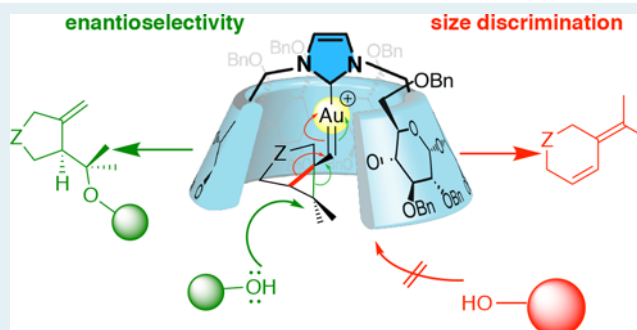
**HAL** is a multi-disciplinary open access archive for the deposit and dissemination of scientific research documents, whether they are published or not. The documents may come from teaching and research institutions in France or abroad, or from public or private research centers.

L'archive ouverte pluridisciplinaire **HAL**, est destinée au dépôt et à la diffusion de documents scientifiques de niveau recherche, publiés ou non, émanant des établissements d'enseignement et de recherche français ou étrangers, des laboratoires publics ou privés.

# $\beta$ -Cyclodextrin–NHC–Gold(I) Complex ( $\beta$ -ICyD)AuCl: A Chiral Nanoreactor for Enantioselective and Substrate-Selective Alkoxy cyclization Reactions

Coralie Tugny,<sup>§</sup> Natalia del Rio,<sup>§</sup> Mehdi Koohgard, Nicolas Vanthuyne, Denis Lesage, Kajetan Bijouard, Pinglu Zhang, Jorge Mejjide Suárez, Sylvain Roland, Etienne Derat, Olivia Bistri-Aslanoff, Matthieu Sollogoub,<sup>\*</sup> Louis Fensterbank,<sup>\*</sup> and Virginie Mouriès-Mansuy<sup>\*</sup>

**ABSTRACT:** NHC-capped  $\beta$ -cyclodextrin ( $\beta$ -ICyD) was used as a ligand for gold-catalyzed alkoxy cyclization reactions. The cavity was found to be responsible for a triple selectivity: (i) the asymmetric shape of the cavity of  $\beta$ -ICyD induced highly stereoselective cyclizations, (ii) the shape of the interior favored the formation of a six-membered ring in the absence of a nucleophile, and finally, (iii) the encapsulation of the metal inside the cavity disfavored the addition of sterically hindered alcohols. Highly enantioselective and substrate-selective alkoxy cyclizations of enynes are therefore promoted by the cavity-based molecular reactor ( $\beta$ -ICyD)AuCl.

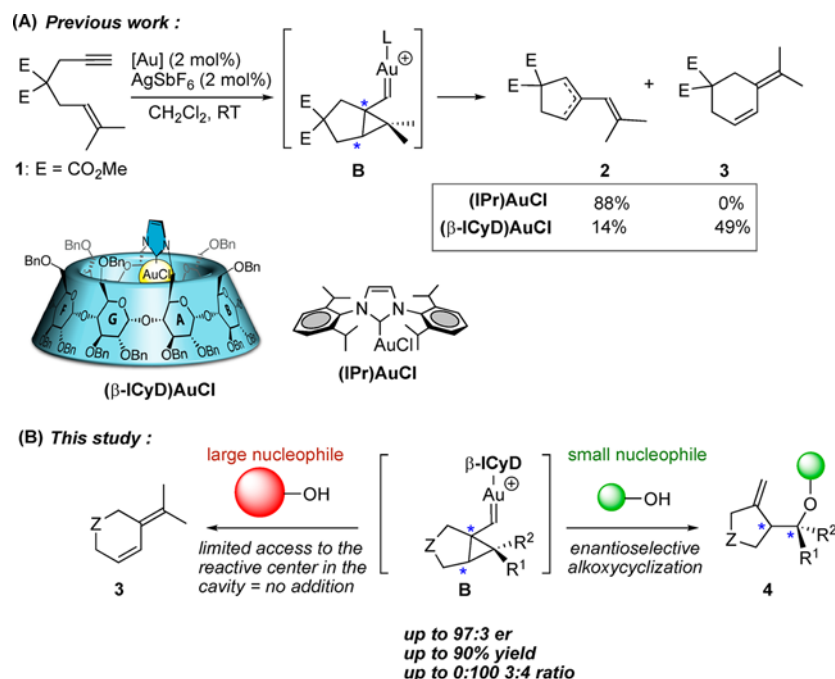


## 1. INTRODUCTION

Gold(I) homogeneous catalysis has become a method of choice in organic synthesis,<sup>1</sup> notably to reach molecular complexity.<sup>2</sup> Numerous applications in the total synthesis of natural products<sup>3</sup> and asymmetric catalysis<sup>4</sup> have been reported. In gold(I) homogeneous catalysis, a wide range of precatalysts having (neutral) L ligands embracing a very diverse set of electronic and steric patterns have been used to generate the generic [LAu]<sup>+</sup> active catalytic species.<sup>5</sup> It has been shown that the nature of the ligand (L) strongly affects the outcome and selectivity of the reactions. Although extensive screening studies and calculations have been performed to gain a better understanding of the ligand effects,<sup>6</sup> it still remains difficult to safely select a ligand for a specific utilization, which suggests that greater efforts have to be devoted to the design of gold salt ligands. The linear coordination of gold(I) allowing free rotation around the L–Au bond adds a particular difficulty in ligand design and makes challenging the control of the gold environment to induce high selectivities in the targeted reactions. Recently, it has been shown that encapsulation of the active gold center constituted an interesting option<sup>7</sup> that has been explored to generate a restricted environment to control different types of selectivities in reactions,<sup>8</sup> such as regioselectivity<sup>9</sup> or variation of product distribution,<sup>10</sup> substrate selectivity,<sup>11</sup> and stabilization of reactive species to favor a specific reaction pathway.<sup>12</sup> In this context, we have developed the use of NHC-capped cyclo-

dextrin (CD) gold(I) complexes denoted ( $\alpha$ -ICyD)AuCl derived from  $\alpha$ -CD and logically ( $\beta$ -ICyD)AuCl for a  $\beta$ -CD-derived complex that both fully encapsulates the metal center while retaining its activity and allowing selective reactions to be performed.<sup>13–16</sup> Importantly, we showed that the asymmetric CD cavity could generate a chiral enough environment around the metal center to induce enantioselective cycloisomerizations with ee values up to 80% with  $\beta$ -ICyD.<sup>13,14</sup> We further evidenced a cavity effect ( $\alpha$ - vs  $\beta$ -CD) in the cycloisomerization of the prototypical enyne system **1** (Scheme 1A). While ( $\alpha$ -ICyD)AuCl and (IPr)AuCl complexes provided the commonly observed cyclopentadienic mixture **2**, the  $\beta$ -ICyD-based complex favored the formation of the cyclohexadiene product **3** and gave the highest yield observed for this compound.<sup>13,14</sup> In this reaction, however, the stereoselectivity that can be obtained in the formation of the chiral gold carbene intermediate **B** in the presence of a chiral ligand is lost in the rearrangement to give achiral cyclic dienes **2** and **3**. Nevertheless, it has been shown that, in the presence of an

**Scheme 1. (A) Change in the Course of the Cycloisomerization Reaction toward the Formation of a Six-Membered Ring by ( $\beta$ -ICyD)AuCl and (B) Inducement of Substrate Selection, Control of Reaction Pathways, and Generation of High Enantioselectivity in the Alkoxy cyclization Reaction by the  $\beta$ -CD Cavity**



external nucleophile such as water or an alcohol, intermediate **B** can be intercepted toward the competitive formation of the alkoxy cyclization product **4**,<sup>17</sup> in which (in contrast to **2** and **3**) the chiral information on **B** is kept and induces the formation of a new stereogenic center. Therefore, in the presence of a chiral ligand the reaction can be enantioselective.<sup>18</sup> We therefore saw in this reaction the opportunity to probe multiple selectivities with the encapsulating asymmetric  $\beta$ -ICyD ligand: enantioselectivity and substrate and product selectivity. We hypothesized that nucleophilic addition on the  $\alpha$ -cyclopropylcarbene intermediate **B** should depend on its accessibility to the nucleophile and, if the cavity of  $\beta$ -ICyD plays its role, modulating the size of the nucleophile should allow controlling the formation of either **3** or **4**, with possible control of the stereoselectivity for **4** (Scheme 1B). Thus, we studied the alkoxy cyclization reaction catalyzed by ( $\beta$ -ICyD)-AuCl using different external nucleophiles and studied whether a modulation of the outcome could be detected. The results and details of this study are presented herein.

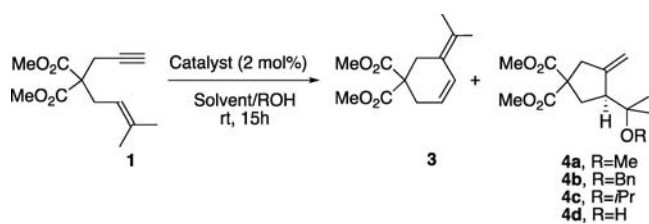
## 2. RESULTS AND DISCUSSION

A methoxycyclization reaction of enyne **1** was therefore studied (Table 1) and run using a 7/3 mixture of MeOH and DCM under standard conditions, where the precatalyst is first activated with a silver salt and the substrate is added to the resulting mixture.<sup>19</sup> Under these conditions, (IPr)AuCl afforded the expected product ( $\pm$ )-**4a** with an excellent yield (98%). When ( $\beta$ -ICyD)AuCl was used, the methoxycyclization product (–)-(S)-**4a**<sup>20</sup> was solely obtained with an excellent enantiomeric ratio (er) (er = 97:3, entry 2, vs 89:11 recently reported with a chiral bifunctional NHC gold(I) complex by Zhang and co-workers).<sup>21</sup> Of note, ( $\beta$ -ICyD)AuCl did not promote the reaction on its own. In the case of a benzylic alcohol as an external nucleophile, the adduct (–)-**4b**<sup>22</sup> was obtained as a single product with a very good er of 92:8 (entry

6). Finally, using a sterically more demanding nucleophile, *i*PrOH, we obtained (–)-**4c**<sup>23</sup> in 53% yield with a moderate er of 73:27 together with 30% of **3** (entry 10). These results tend to show that the size of the nucleophile indeed matters, as *i*PrOH is the largest alcohol and is also the least efficient nucleophile. In these reactions, the order of addition of the silver salt is sometimes important.<sup>23</sup> We therefore mixed all components of the reaction but the silver salt, which we added after 5 min (entries 3, 7, and 11). Interestingly, in this case, for BnOH and *i*PrOH the amount of cyclohexene **3** increased significantly. In fact, when *i*PrOH was used, **3** was almost the exclusive product (entry 11). In order to also check the influence of the silver salt in this reaction,<sup>23–25</sup> we decided to use a silver-free cationic gold catalyst.<sup>26</sup> To this end, we treated ( $\beta$ -ICyD)AuCl with 1 equiv of AgNTf<sub>2</sub> and obtained the ( $\beta$ -ICyD)AuNTf<sub>2</sub> complex in 87% yield after filtration over a Millipore filter (0.20  $\mu$ m). The mass analysis of the mother liquor showed that all the silver salts were removed, thanks to the filtration over a Millipore filter, as reported by Shi.<sup>24</sup> When this catalyst was used, the results were similar to those obtained when the silver salt was mixed with ( $\beta$ -ICyD)AuCl before adding the substrate. All of these results seem to show that the most important parameter to have good selectivity is to add the substrate once the gold complex is cationic. For the gold lying inside the cyclodextrin we observe again a significant cavity effect and not a silver salt effect.

We finally examined the addition of water by using a 7/1 mixture of dioxane and water.<sup>18,27</sup> With (IPr)AuCl as the precatalyst, ( $\pm$ )-**4d** was obtained as the sole product resulting from the nucleophilic addition of water onto the carbene-like intermediate (Table 1, entry 13). It is worth noting that the reaction with ( $\beta$ -ICyD)AuCl provided the expected hydroxycyclization product (–)-**4d**<sup>20</sup> predominantly but always with around 10% of cyclohexadiene **3** (entries 14–16). The reaction was efficient in terms of enantioinduction,<sup>18–21</sup> as

**Table 1. Enantioselective Hydroxycyclization and Alkoxy cyclization Reactions<sup>a</sup>**



entry	catalyst	R	yield <sup>h</sup> (%) (er) <sup>i</sup>	
			3	4
1 <sup>b</sup>	(IPr)AuCl	Me		4a: 98
2 <sup>b</sup>	( $\beta$ -ICyD)AuCl	Me		4a: 95 (97:3) (–)
3 <sup>c</sup>	( $\beta$ -ICyD)AuCl	Me		4a: 57 (96:4)
4 <sup>d</sup>	( $\beta$ -ICyD)AuNTf <sub>2</sub>	Me		4a: 77 (95:5) (–)
5 <sup>b</sup>	(IPr)AuCl	Bn		4a: 90
6 <sup>b</sup>	( $\beta$ -ICyD)AuCl	Bn		4b: 90 (92:8) (–)
7 <sup>c</sup>	( $\beta$ -ICyD)AuCl	Bn	25	4b: 60 (75:25) (–)
8 <sup>d</sup>	( $\beta$ -ICyD)AuNTf <sub>2</sub>	Bn	12	4b: 69 (88:12) (–)
9 <sup>b</sup>	(IPr)AuCl	iPr		4c: 86
10 <sup>b</sup>	( $\beta$ -ICyD)AuCl	iPr	30	4c: 53 (73:27)
11 <sup>c</sup>	( $\beta$ -ICyD)AuCl	iPr	77	4c: 7 (ND)
12 <sup>d</sup>	( $\beta$ -ICyD)AuNTf <sub>2</sub>	iPr	12	4c: 51 (93:7) (–)
13 <sup>e</sup>	(IPr)AuCl	H		4d: >99
14 <sup>e</sup>	( $\beta$ -ICyD)AuCl	H	10	4d: 51 (93:7) (–)
15 <sup>f</sup>	( $\beta$ -ICyD)AuCl	H	12	4d: 42 (94:6) (–)
16 <sup>g</sup>	( $\beta$ -ICyD)AuNTf <sub>2</sub>	H	10	4d: 61 (94:6) (–)

<sup>a</sup>All experiments were performed at 0.05 mol/L. <sup>b</sup>Substrate **1** in DCM was added to a mixture of LAuCl (2 mol %) and AgSbF<sub>6</sub> (2 mol %) in ROH (ROH/DCM 7/3 v/v). <sup>c</sup>AgSbF<sub>6</sub> in DCM (2 mol %) was added to a mixture of ( $\beta$ -ICyD)AuCl (2 mol %) and substrate **1**, in ROH/DCM (7/3 v/v). <sup>d</sup>ROH/DCM (7/3 v/v). <sup>e</sup>Substrate **1** was added to a mixture of LAuCl (2 mol %) and AgSbF<sub>6</sub> (2 mol %) in dioxane/H<sub>2</sub>O (7/1 v/v). <sup>f</sup>AgSbF<sub>6</sub> in dioxane (2 mol %) was added to a mixture of ( $\beta$ -ICyD)AuCl (2 mol %) and substrate **1**, in dioxane/H<sub>2</sub>O (7/1 v/v). <sup>g</sup>Dioxane/H<sub>2</sub>O (7/1 v/v). <sup>h</sup>Isolated yields. <sup>i</sup>er values were determined using chiral HPLC.

(–)-**4d** was obtained with an er of 94:6 (vs 83:17 reported for the same substrate by Michelet and co-workers with Pt<sup>18a</sup>). For this reaction, adding the silver salt after the substrate or using ( $\beta$ -ICyD)AuNTf<sub>2</sub> did not significantly change the outcome of the reaction (entries 15 and 16).

From this first set of experiments, a striking difference in behavior between IPr and  $\beta$ -ICyD ligands is observed. With IPr the sole product of the reaction is the alkoxy cyclization product, and with  $\beta$ -ICyD a competition between this alkoxy cyclization and formation of the 6-endo-dig compound **3** occurs. Furthermore, with the cavity substrate selectivity seems to occur, as MeOH always gives the alkoxy cyclization product **4d**, while *i*PrOH looks more prone to give the cyclohexene **3**. In this series, however, the behavior of water seems surprising, as it should be a smaller nucleophile and therefore should preferentially take the hydroxycyclization pathway. To probe the substrate selectivity of our system, we therefore decided to compare the different external nucleophiles against MeOH by realizing a competition assay. When MeOH and BnOH are used in an equimolar ratio,  $\beta$ -ICyD does not make a difference between the two, as a similar ratio of both alkoxy cyclized products is obtained (Table 2, entry 2). In the competition between MeOH and *i*PrOH, the formation of the methanol adduct (**4a**) was only slightly favored with

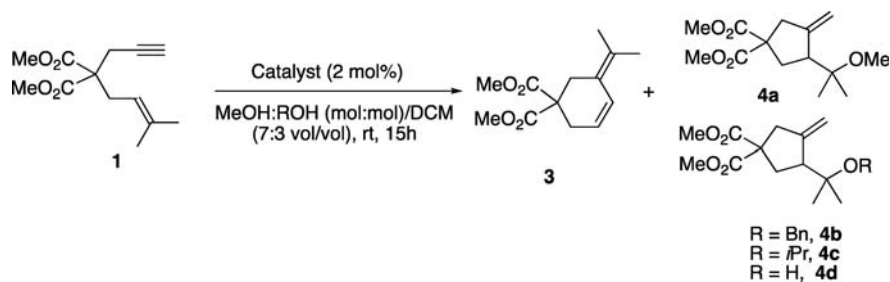
(IPr)AuCl (entry 4), but the  $\beta$ -ICyD environment (entry 5) significantly increased this trend, since the selectivity factor increased by a factor of 10. Finally, with the H<sub>2</sub>O/MeOH mixture, (IPr)AuCl led to the preferred addition of MeOH with a selectivity of 2.4. When ( $\beta$ -ICyD)AuCl was used as a precatalyst, the cyclohexene **3** was isolated in 30% yield and methoxycyclization compound **4a** was obtained with a good selectivity of 11.2 in comparison to its hydroxylated counterpart **4d** (entry 8). It therefore seems that water in this system is not as good a nucleophile as MeOH, which explains why, when it is used by itself, it allows the competitive formation of a significant quantity of cyclohexene **3** (Table 1, entries 15 and 16). This is probably linked to the hydrophobicity of the CD cavity. As previously observed, the addition of the silver salts prior to that of the substrate slightly favors the alkoxy cyclization pathway (Table 2, entries 1, 2, 4, 5, 7, and 8). Of note also, (IPr)AuCl never gives **3** in these series of reactions.

To expand the scope of our study, we looked at N-tethered 1,6-enynes. With these substrates the selectivity of the reaction is total toward the alkoxy cyclization pathway, as we never observed the corresponding cycloisomerized dienes. Enyne **5a**, with a prenyl moiety, underwent enantioselective methoxycyclization to give product (–)-**6a**<sup>22</sup> in good yield and very high er values (92:8 to 94:6) never reported in the literature<sup>21</sup> (Table 3, entries 2 and 3). Furthermore, with enyne **5b** having a (*E*)-styryl moiety and a terminal alkyne, the expected alkoxy cyclization product (–)-**6b**<sup>20</sup> was obtained in quite a good yield and with again a good er,<sup>18–21</sup> 93:7 to 94:6 (entries 5 and 6, vs. 89:11 reported by Michelet and co-workers with Pt).<sup>18a</sup>

We then sought for a rationale of these results. The first step in the mechanism is the A  $\rightarrow$  B cyclization which corresponds to the first stereodetermining step (Scheme 2). We previously showed that the shape of the cavity could account for the selectivities observed with the ICyD ligand.<sup>14,15</sup> In particular, we could rationalize the enantioselectivity of another gold-catalyzed cycloisomerization on the basis of the proposed shape of the cavity.<sup>14</sup> Hence, the same technique was applied here using either the previously modeled shape or a simplified version of it, where the triangles represent the sugar units and their color reflecting their proximity with the reactive center (the darker the closer) (Scheme 2). We then hypothesized that in the present case the C(CO<sub>2</sub>Me)<sub>2</sub> group is the most sterically demanding and therefore its position in the flatter area of the cavity should be favored. The enyne folds so that the alkene can approach the activated alkyne to form the cyclopropane in two different manners that will result in the two enantiomers. As can be seen from Scheme 2, in one case the *gem*-dimethyl is next to the wall of the cavity and in the other case it is in the middle of the cavity. This latter approach should therefore be favored. Rewardingly, using this model we found that this approach is indeed leading to the major enantiomer. The second step of the alkoxy cyclization reaction is the addition of the external nucleophile. When a small and good nucleophile is used (in green), its addition to the  $\alpha$ -cyclopropylcarbene intermediate **B** is presumably fast, leading to the exclusive formation of the alkoxy cyclization products **4** or **6** (green pathway). In contrast, when a larger nucleophile is used (red), its addition to the gold  $\alpha$ -cyclopropylcarbene **B** is disfavored, and the latter more rapidly evolves toward the competitive formation of the cyclized compound **3** (Scheme 2), which results from a double-cleavage process of **B** (blue pathway).<sup>28</sup> We previously showed that the  $\beta$ -ICyD cavity favored the conformation of the  $\alpha$ -cyclopropylcarbene **B** depicted in



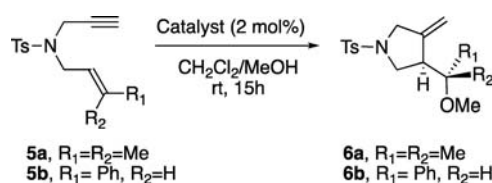
**Table 2. Competitive Alkoxy cyclizations<sup>a</sup>**



entry	catalyst	R	yield (%) <sup>d</sup>			S factor 4a:4x
			3	4a	4x	
1 <sup>b</sup>	(IPr)AuCl	Bn		53	4b: 27	1.9
2 <sup>b</sup>	( $\beta$ -ICyD)AuCl	Bn	29	39	4b: 32	1.2
3 <sup>c</sup>	( $\beta$ -ICyD)AuCl	Bn	30	28	4b: 35	0.8
4 <sup>b</sup>	(IPr)AuCl	iPr		58	4c: 42	1.4
5 <sup>b</sup>	( $\beta$ -ICyD)AuCl	iPr	12	79	4c: 8	9.9
6 <sup>c</sup>	( $\beta$ -ICyD)AuCl	iPr	30	50	4c: 10	10
7 <sup>b</sup>	(IPr)AuCl	H		41	4d: 17	2.4
8 <sup>b</sup>	( $\beta$ -ICyD)AuCl	H	30	56	4d: 5	11.2
9 <sup>c,e</sup>	( $\beta$ -ICyD)AuCl	H	20	23	4d: 5	4.6

<sup>a</sup>All experiments were performed at 0.05 mol/L. <sup>b</sup>Substrate **1** in DCM was added to a mixture of LAuCl (2 mol %) and AgSbF<sub>6</sub> (2 mol %) in MeOH:ROH (1/1 mol ratio), (MeOH:ROH/DCM 7/3 v/v). <sup>c</sup>AgSbF<sub>6</sub> in DCM (2 mol %) was added to a mixture of ( $\beta$ -ICyD)AuCl (2 mol %) and substrate **1**, in MeOH:ROH (1/1 mol ratio), MeOH:ROH/DCM (7/3 v/v). <sup>d</sup>Isolated yields. <sup>e</sup>40% of **1** is recovered.

**Table 3. Alkoxy cyclizations with N-Tethered Enynes<sup>a</sup>**



entry	catalyst	R <sup>1</sup>	R <sup>2</sup>	yield (%) <sup>d</sup> (er) <sup>e</sup> <b>6</b>
1 <sup>b</sup>	(IPr)AuCl	Me	Me	60
2 <sup>b</sup>	( $\beta$ -ICyD)AuCl	Me	Me	79 (92:8) (–)
3 <sup>c</sup>	( $\beta$ -ICyD)AuNTf <sub>2</sub>	Me	Me	71 (94:6) (–)
4 <sup>b</sup>	(IPr)AuCl	Ph	H	55
5 <sup>b</sup>	( $\beta$ -ICyD)AuCl	Ph	H	58 (93:7) (–)
6 <sup>c</sup>	( $\beta$ -ICyD)AuNTf <sub>2</sub>	Ph	H	73 (94:6) (–)

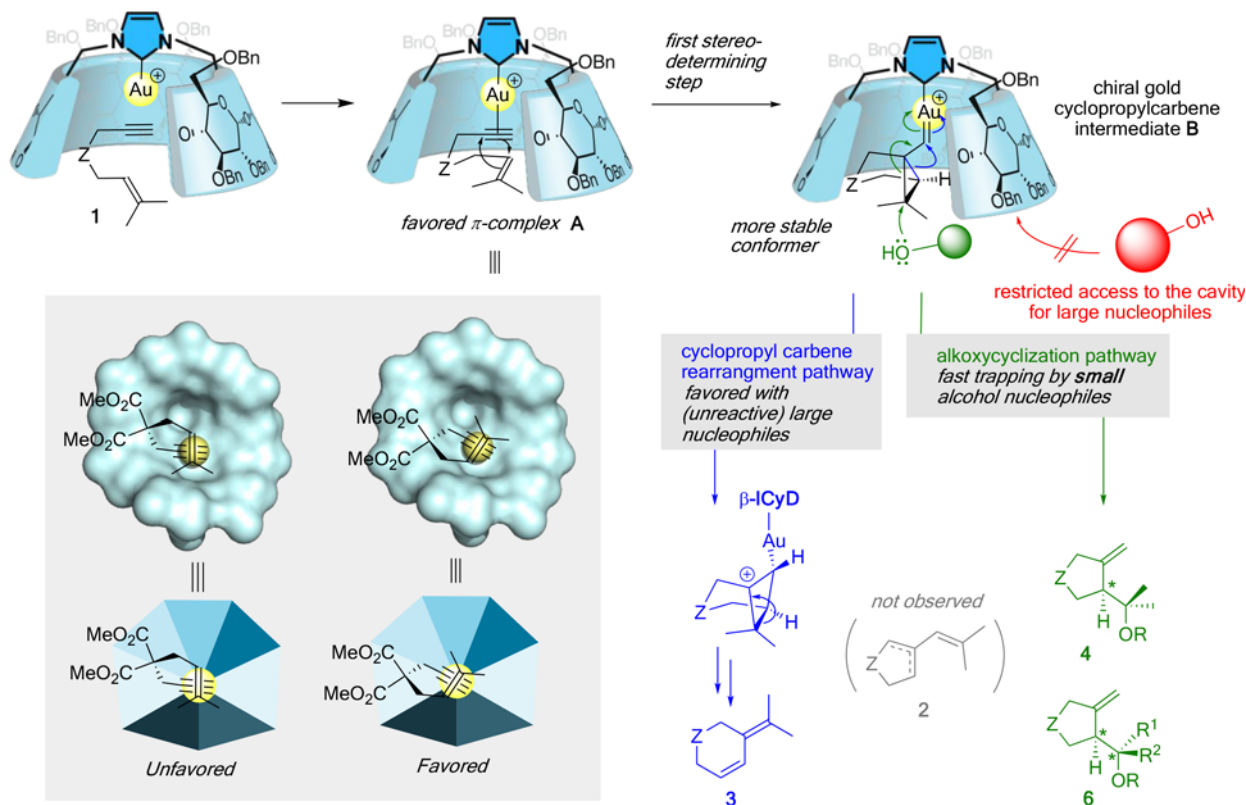
<sup>a</sup>All experiments were performed at 0.05 mol/L. <sup>b</sup>Substrate **1** in DCM was added to a mixture of LAuCl (2 mol %) and AgSbF<sub>6</sub> (2 mol %) in MeOH (MeOH/DCM (7/3 v/v)). <sup>c</sup>MeOH/DCM (7/3 v/v). <sup>d</sup>Isolated yield. <sup>e</sup>er values were determined using chiral HPLC.

**Scheme 2** leading to the six-membered product **3** rather than the five-membered compound **2** through a less favored conformation of **B**.<sup>14</sup>

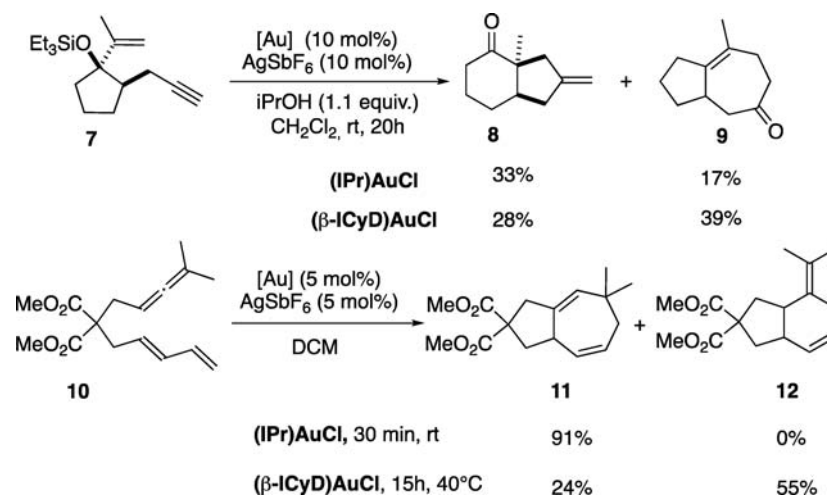
At this stage, it seems difficult to rationalize the effect of the order of addition of the silver salt on the selectivity of the reaction. Nevertheless, it appears as a general trend from **Tables 1** and **2** that precatonization (AgSbF<sub>6</sub> added first) leads to better yields of alkoxy cyclization or hydroxycyclization with decreased formation of **3** in comparison to those when AgSbF<sub>6</sub> is added last. Interestingly also, the cationic complex ( $\beta$ -ICyD)AuNTf<sub>2</sub> appears to lie between these two situations with sometimes a reactivity close to or even better than in the precatonization scenario (**Table 1**, entry 12 vs 10 or entry 16 vs 14). The NTf<sub>2</sub><sup>–</sup> counterion must have some influence as well.

In the case of alkoxy cyclization, when AgSbF<sub>6</sub> is added first, the anion metathesis on gold takes place only in the alcohol (MeOH, BnOH, *i*PrOH, H<sub>2</sub>O).<sup>29</sup> Even though we have never observed any ( $\beta$ -ICyD)Au(ROH)<sup>+</sup> adduct by MS, we can assume that ROH must form a first solvation shell around the cationic gold species by polar interaction. To give some support to this hypothesis, we decided to perform some tight-binding density functional calculations, using the xtb software<sup>30</sup> and the GFN2-xTB method<sup>31</sup> developed by the Grimme group. This computational method was recently used to describe binding in supramolecular chemistry.<sup>32</sup> By performing a molecular dynamics on the system ( $\beta$ -ICyD)-AuCl solvated by methanol molecules, taken as a model ROH, we found that up to four molecules of MeOH can sit in the cavity, with two molecules of methanol interacting directly by hydrogen bonding with the chloride. When the gold atom sitting in the cavity was now cationic, we found five molecules of methanol around it, one of them interacting directly with the metallic center. It is also known from the literature that in a binary solution of solvents which differ in their polarity and their protic properties (here CH<sub>2</sub>Cl<sub>2</sub> and ROH), the statistical average weight of the protic solvent in the first solvation shell of a cation will be higher than that in the bulk mixture.<sup>33</sup> Thus, after addition of the substrate in dichloromethane, assuming that the interaction of the cationic gold species with CH<sub>2</sub>Cl<sub>2</sub> is weak, ROH molecules would remain close to the carbene intermediate **B**, leading to the formation of **4**. This is supported by DFTB calculations, which show that after a 50 ps molecular dynamics of ( $\beta$ -ICyD)AuCl in a solvent mixture of methanol and CH<sub>2</sub>Cl<sub>2</sub>, two molecules of methanol remain in interaction with the metallic moiety while two molecules of CH<sub>2</sub>Cl<sub>2</sub> are sitting at the entrance of the CD cavity, in stacking with the benzylic groups. Interestingly also, our calculations show that the barrier of extrusion of MeOH is higher with cationic gold (11.14 kcal/mol) than with a neutral species (6.23 kcal/mol) (see the [Supporting Information](#) for details).

Scheme 2. Proposed Rationale for the Observed Selectivities



Scheme 3. Diagnostic Cycloisomerizations



At the other end, with *i*PrOH the formation of **3** increased (see Table 1, entries 10–12) presumably because of the size and the constraints imposed by the cavity, and so the interactions with cationic gold are weaker. This effect was reinforced when the silver salt was introduced later (Table 1, entry 11, 77% of **3**). We decided to investigate this point by performing molecular dynamics at the DFTB level with two different starting conditions: either from (β-ICyD)AuCl or from (β-ICyD)Au<sup>+</sup>. The radial pair distribution function between gold and oxygen atoms was calculated (see Figure S2 in the Supporting Information). While in the case of Au<sup>+</sup>, one *i*PrOH can nearly always be found around 2.2 Å of the gold atom, this probability is much lower in the case of AuCl. From these data, we can submit the hypothesis that the outcome of the catalysis

is dependent on the initial conditions which are influencing the solvation sphere around gold.

The competitive experiments of Table 2 seem to favor the formation of **3** at the expense of adducts **4**. This is especially true for entries 2 and 3, where around 30% of **3** is formed, while with MeOH or BnOH alone, no **3** or little **3** is formed (Table 1, entries 1–8), as though the 1/1 mixture of MeOH and BnOH was more sterically demanding than each of the separate solvents. This observation also holds with H<sub>2</sub>O as a nucleophile. The MeOH/H<sub>2</sub>O mixture is less trapped, resulting in more **3** in Table 2. In the case of *i*PrOH/MeOH (entries 5 and 6), the results are more consistent, since the proportion of **3** is much weaker than that with *i*PrOH (Table 1, entries 10–12). In that case, the trapping of MeOH reduces

the amount of **3**. However, the reduction is not total, since there is roughly half as much MeOH under the conditions of Table 2. Thus, mixing alcohols appears to alter the physicochemical properties of the alcohol or water taken alone and thus their intrinsic reactivity.<sup>34</sup>

We based all our reasoning on the sole influence of the cavity, in comparing ICyD with IPr, but an electronic factor could also be at play. For geometrical reasons, the orbitals of the nitrogen atoms on the NHC might not be conjugated with the carbene and this would induce a change in its properties as demonstrated by Bertrand.<sup>35</sup> We therefore decided to probe the electronic properties of our carbene with two diagnostic reactions and a spectroscopic method. In the cycloisomerization of enyne **7**, electron-rich ligands favor a pinacol type of rearrangement from the  $\alpha$ -cyclopropyl intermediate leading to product **8**, while electron-poor ligands trigger a [3,3]-sigmatropic rearrangement leading to cycloheptenone **9** (Scheme 3).<sup>36</sup> Hence, electron-rich IPr logically reacted toward the preferential formation of **8**. In contrast, the selectivity of the reaction was reversed toward the formation of **9** with ( $\beta$ -ICyD)AuCl as the precatalyst.  $\beta$ -ICyD gold complexes thus behave in this reaction like catalysts bearing significantly less electron donating ligands. This could also suggest an appreciable  $\pi$ -acceptor character. Furthermore, allenediene **10** also appeared as a valuable probe, since electron-rich ligands favor the formation of [4 + 3] cycloadducts of type **11** through the intervention of a carbene type reactivity, in contrast to electron-poor ligands which trigger a cationic event leading to the formal [4 + 2] cycloadduct **12** originating from a Wagner–Meerwein rearrangement. While the cyclization of **10** smoothly took place with both carbene gold complexes, a contrasting selectivity was observed between them. IPr selectively led to the formation of adduct **11**, while  $\beta$ -ICyD afforded a 2.3 ratio of [4 + 2] **12**/[4 + 3] **11**, a ratio close to that observed by Fürstner with a good  $\pi$ -acceptor carbene ligand (Scheme 3).<sup>36b,37</sup>

This set of results suggests that an electronic bias could be at play in these cycloisomerization reactions. We therefore also evaluated the electronic properties of the  $\beta$ -ICyD ligand by measuring the <sup>77</sup>Se NMR chemical shift of ( $\beta$ -ICyD)Se to assess its  $\pi$ -accepting ability.<sup>38</sup> The ( $\beta$ -ICyD)Se adduct was synthesized according to a literature procedure.<sup>38</sup> With a signal at  $\delta$  62 ppm (acetone-*d*<sub>6</sub>) in <sup>77</sup>Se NMR, the selenourea ( $\beta$ -ICyD)Se exhibits a rather strong  $\pi$ -donor character, similar to that of IPr carbene (IPr-Se,  $\delta$  87 ppm).<sup>39,38b</sup> Thus, the electronic properties of  $\beta$ -ICyD carbene being similar to those of IPr, the difference in reactivity can be solely attributed to the cavity.

We have once more shown the great influence of the cavity of the CD could have when it is capped with an NHC in ICyD. The influence in the reaction of alkoxy cyclization is 3-fold: (i) the asymmetric shape of the cavity of  $\beta$ -ICyD induces a stereoselective cyclization, (ii) the shape of the interior favors the formation of a six-membered ring in the absence of a nucleophile, and finally, (iii) the encapsulation of the metal inside the cavity disfavors the addition of sterically hindered alcohols.

In summary, the cavity in the  $\beta$ -ICyD-based catalytic system exerts a strong influence in alkoxy cyclization reactions. The asymmetric shape of the cavity of these chiral nanoreactors induces highly stereoselective transformations, providing in some cases the highest observed *er* values so far for this

reaction. While the formation of a six-membered ring in the absence of alcohols as external nucleophiles is observed, this outcome being dictated as well by the shape of the cavity, the constrained environment of the metal inside  $\beta$ -ICyD also allows discriminations in the alcohol addition process by size exclusion or hydrophobic effects. Finally,  $\beta$ -ICyD is an NHC-based catalyst whose determined electronic factors are consistent with a strongly electron donating NHC but whose reactivity in some cases is reminiscent of gold catalysts bearing electron-depleted ligands. This reactivity paradigm shift can also be imputed to the influence of the cavity. All in all, the cavity shape is the main element explaining the multiple selectivities observed here, very much as in metallo-enzymes.

(1) (a) *Homogenous Gold Catalysis*; Michelet, V., Toste, F. D., Eds.; Imperial College Press: London, 2014. (b) *Modern Gold Catalysis Synthesis*; Hashmi, A. S. K., Toste, F. D., Eds.; Wiley: 2012.

(2) (a) Fensterbank, L.; Malacria, M. Molecular complexity from polyunsaturated substrates: the gold catalysis approach. *Acc. Chem. Res.* **2014**, *47*, 953–965. (b) Dorel, R.; Echavarren, A. M. Gold(I)-Catalyzed Activation of Alkynes for the Construction of Molecular Complexity. *Chem. Rev.* **2015**, *115*, 9028–9072.

(3) For reviews on the use of gold catalysis in total synthesis, see: (a) Mato, M.; García-Morales, C.; Echavarren, A. M. Generation of Gold(I) Carbenes by Retro-Buchner reactions: From Cyclopropanes to Natural Products Synthesis. *ChemCatChem* **2019**, *11*, 53–72. (b) Quach, R.; Furkert, D. P.; Brimble, M. A. Gold catalysis: synthesis of spiro, bridged, and fused natural products. *Org. Biomol. Chem.* **2017**, *15*, 3098–3104. (c) Pflästerer, D.; Hashmi, A. S. K. Gold catalysis in total synthesis – recent achievements. *Chem. Soc. Rev.* **2016**, *45*, 1331–1367. (d) Zhang, Y.; Luo, T.; Yang, Z. Strategic innovation in the total synthesis of complex natural products using gold catalysis. *Nat. Prod. Rep.* **2014**, *31*, 489–503. For some recent contributions, see: (e) Miloserdov, F. M.; Kirillova, M. S.; Muratore, M. E.; Echavarren, A. M. Unified Total Synthesis of Pyrroloazocine Indole Alkaloids Sheds Light on Their Biosynthetic Relationship. *J. Am. Chem. Soc.* **2018**, *140*, 5393–5400. (f) Dorel, R.; Echavarren, A. M. Ready Access to the Echinopines Skeleton via Gold(I)-Catalyzed Alkoxy cyclization of Enynes. *J. Org. Chem.* **2016**, *81*, 8444–8454. (g) Pflästerer, D.; Rudolph, M.; Yates, B. F.; Ariafard, A.; Hashmi, A. S. K. Total Synthesis of (±)-Dihydroisobamamol. *Adv. Synth. Catal.* **2017**, *359*, 866–874. (h) McGee, P.; Bétournay, G.; Barabé, F.; Barriault, L. A 11-Steps Total Synthesis of Magellanine through a

Gold(I)-Catalyzed Dehydro Diels-Alder Reaction. *Angew. Chem., Int. Ed.* **2017**, *56*, 6280–6283.

(4) For reviews on asymmetric induction in gold catalysis, see: (a) Pradal, A.; Toullec, P. Y.; Michelet, V. Recent Developments in Asymmetric catalysis in the Presence of Chiral Gold Complexes. *Synthesis* **2011**, *2011*, 1501–1514. (b) Watson, I. D. G.; Toste, F. D. Catalytic enantioselective carbon-carbon bond formation using cycloisomerization reactions. *Chem. Sci.* **2012**, *3*, 2899–2919. (c) Wang, Y.-M.; Lackner, A. D.; Toste, F. D. Development of catalysts and ligands for enantioselective gold catalysis. *Acc. Chem. Res.* **2014**, *47*, 889–901. (d) Zi, W.; Toste, D. F. Recent advances in enantioselective gold catalysis. *Chem. Soc. Rev.* **2016**, *45*, 4567–4589. (e) López, F.; Mascareñas, J. L. Gold(I)-catalyzed enantioselective cycloaddition reactions. *Beilstein J. Org. Chem.* **2013**, *9*, 2250–2264.

(5) Ranieri, B.; Escofet, I.; Echavarren, A. M. Anatomy of gold catalyst: facts and myths. *Org. Biomol. Chem.* **2015**, *13*, 7103–7118.

(6) (a) Wang, W.; Hammond, G. B.; Xu, B. Ligands Effects and Ligand Design in Homogeneous Gold(I) Catalysis. *J. Am. Chem. Soc.* **2012**, *134*, 5697–5705. For reviews on ligand effects in gold catalysis, see: (b) Gorin, D. J.; Sherry, B. D.; Toste, F. D. Ligand effects in homogeneous Au catalysis. *Chem. Rev.* **2008**, *108*, 3351–3378. (c) Wang, Y.-M.; Lackner, A. D.; Toste, F. D. Development of catalyst and ligands for enantioselective gold catalysis. *Acc. Chem. Res.* **2014**, *47*, 889–901.

(7) (a) Hong, C. M.; Bergman, R. G.; Raymond, K. N.; Toste, F. D. Self-assembled tetrahedrals hosts as supramolecular catalysts. *Acc. Chem. Res.* **2018**, *51*, 2447–2455. (b) Leenders, S. H. A. M.; Gramage-Doria, R.; de Bruin, B.; Reek, J. N. H. Transition metal catalysis in confined spaces. *Chem. Soc. Rev.* **2015**, *44*, 433–448. (c) Jans, A. C. H.; Caumes, X.; Reek, J. N. H. Gold Catalysis in (Supra) Molecular Cages to Control Reactivity and Selectivity. *ChemCatChem* **2019**, *11*, 287–297.

(8) (a) Heard, A.; Goldup, S. A Mechanically Planar Chiral Rotaxane Ligand for Enantioselective Catalysis. *Chem.* **2020**, *6*, 994. (b) Galli, M.; Lewis, J. E. M.; Goldup, S. M. A Stimuli-responsive Rotaxane-Gold Catalyst: Regulation of Activity and Diastereoselectivity. *Angew. Chem., Int. Ed.* **2015**, *54*, 13545–13549. (c) Zuccarello, G.; Mayans, J. G.; Escofet, I.; Scharnagel, D.; Kirillova, M. S.; Pérez-Jimeno, A. H.; Calleja, P.; Boothe, J. R.; Echavarren, A. M. Enantioselective Folding of Enynes by Gold(I) Catalyst with a Remote C<sub>2</sub>-Chiral Element. *J. Am. Chem. Soc.* **2019**, *141*, 11858–11863.

(9) Ho, T. D.; Schamm, M. P. Au-Cavitand Catalyzed Alkyne-Acid Cyclizations. *Eur. J. Org. Chem.* **2019**, *2019*, 5678–5684.

(10) (a) Cavarzan, A.; Scarso, A.; Sgarbossa, P.; Strukul, G.; Reek, J. N. H. Supramolecular control on chemo- and regioselectivity via encapsulation of (NHC)-Au catalyst within a hexameric self-assembled host. *J. Am. Chem. Soc.* **2011**, *133*, 2848–2851. (b) Gramage-Doria, R.; Hessels, J.; Leenders, S. H. A. M.; Tröppner, O.; Dürr, M.; Ivanović-Burmazović, I.; Reek, J. N. H. Gold(I) Catalysis at Extreme Concentration Inside Self-Assembled Nanospheres. *Angew. Chem., Int. Ed.* **2014**, *53*, 13380–13384. (c) Leenders, S. H. A. M.; Dürr, M.; Ivanovic-Burmazovic, I.; Reek, J. N. H. Gold Functionalized Platinum M<sub>12</sub>L<sub>24</sub>-Nanospheres and Their Application in Cyclization Reactions. *Adv. Synth. Catal.* **2016**, *358*, 1509–1518. (d) Endo, N.; Kanaura, M.; Schramm, M. P.; Iwasawa, T. An Introverted Bis-Au Cavitand and its Catalytic Dimerization of Terminal Alkynes. *Eur. J. Org. Chem.* **2016**, *2016*, 2514–2521. (e) Kanaura, M.; Endo, N.; Schramm, M. P.; Iwasawa, T. Evaluation of the Reactivity of Metallocatalytic Cavities in the Dimerization of Terminal Alkynes. *Eur. J. Org. Chem.* **2016**, *2016*, 4970–4975. (f) Jans, A. C. H.; Gómez-Suárez, A.; Nolan, S. P.; Reek, J. N. H. A Switchable Gold Catalyst by Encapsulation in a Self-Assembled Cage. *Chem. - Eur. J.* **2016**, *22*, 14836–14839. (g) Endo, N.; Inoue, M.; Iwasawa, T. Rational Design of a Metallocatalytic Cavitand for Regioselective Hydration of Specific Alkynes. *Eur. J. Org. Chem.* **2018**, *2018*, 1136–1140.

(11) Cavarzan, A.; Reek, J. N. H.; Trentin, F.; Scarso, A.; Strukul, G. Substrate selectivity in the alkyne hydration mediated by NHC-Au(I)



controlled by encapsulation of the catalyst within a hydrogen bonded hexameric host. *Catal. Sci. Technol.* **2013**, 3, 2898–2901.

(12) (a) Wang, Z. J.; Brown, C. J.; Bergman, R. G.; Raymond, K. N.; Toste, F. D. Hydroalkoxylation Catalyzed by a Gold(I) Complex Encapsulated in a Supramolecular Host. *J. Am. Chem. Soc.* **2011**, 133, 7358–7360. (b) Kaphan, D. M.; Levin, M. D.; Bergman, R. G.; Raymond, K. N.; Toste, F. D. A supramolecular microenvironment strategy for transition metal catalysis. *Science* **2015**, 350, 1235–1238. (c) Levin, M. D.; Kaphan, D. M.; Hong, C. M.; Bergman, R. G.; Raymond, K. N.; Toste, F. D. Scope and mechanism of cooperativity at the intersection of organometallic and supramolecular catalysis. *J. Am. Chem. Soc.* **2016**, 138, 9682–9693.

(13) Guitet, M.; Zhang, P.; Marcelo, F.; Tugny, C.; Jimenez-Barbero, J.; Buriez, O.; Amatore, C.; Mouriès-Mansuy, V.; Goddard, J.-P.; Fensterbank, L.; Zhang, Y.; Roland, S.; Ménand, M.; Sollogoub, M. NHC-capped cyclodextrin (ICyDs): insulated metal complexes, commutable multicoordination sphere, and cavity-depend catalysis. *Angew. Chem., Int. Ed.* **2013**, 52, 7213–7218.

(14) Zhang, P.; Tugny, C.; Meijide Suárez, J.; Guitet, M.; Derat, E.; Vanthuyne, N.; Zhang, Y.; Bistri, O.; Mouriès-Mansuy, V.; Ménand, M.; Roland, S.; Fensterbank, L.; Sollogoub, M. Artificial chiral metallo-pockets including a single metal serving as structural probe and catalytic center. *Chem.* **2017**, 3, 174–191.

(15) For cavity-dependent regioselective copper catalysis using the ICyD ligand see also: (a) Zhang, P.; Meijide Suarez, J.; Driant, T.; Derat, E.; Zhang, Y.; Ménand, M.; Roland, S.; Sollogoub, M. Cyclodextrin Cavity-Induced Mechanistic Switch in Copper-Catalyzed Hydroboration. *Angew. Chem.* **2017**, 129, 10961–10965. (b) Wen, Z.; Zhang, Y.; Roland, S.; Sollogoub, M. Carboboration of Alkynes with Cyclodextrin-Encapsulated N-Heterocyclic Carbene Copper Complexes. *Eur. J. Org. Chem.* **2019**, 2019, 2682–2687. (c) Xu, G.; Leloux, S.; Zhang, P.; Meijide Suárez, J.; Zhang, Y.; Derat, E.; Ménand, M.; Bistri-Aslanoff, O.; Roland, S.; Leyssens, T.; Riant, O.; Sollogoub, M. Capturing the Monomeric (L)CuH in NHC-Capped Cyclodextrin: Cavity-Controlled Chemoselective Hydrosilylation of  $\alpha,\beta$ -Unsaturated Ketones. *Angew. Chem., Int. Ed.* **2020**, 59, 7591.

(16) For an identical design see: Kaya, Z.; Andna, L.; Matt, D.; Bentouhami, E.; Djukic, J.-P.; Armspach, D. Benzimidazolium- and Benzimidazolilydene-Capped Cyclodextrins: New Perspectives in Anion Encapsulation and Gold-Catalyzed Cycloisomerization of 1,6-Enynes. *Chem. - Eur. J.* **2018**, 24, 17921–17926.

(17) (a) Méndez, M.; Muñoz, M. P.; Echavarren, A. M. Platinum-Catalyzed Alkoxy- and Hydroxycyclization of Enynes. *J. Am. Chem. Soc.* **2000**, 122, 11549–11550. (b) Nieto-Oberhuber, C.; Nevado, C.; Cárdenas, D. J.; Echavarren, A. M. Cationic Gold(I) Complexes: Highly Alkynophilic Catalysts for the *exo*- and *endo*-Cyclization of Enynes. *Angew. Chem., Int. Ed.* **2004**, 43, 2402–2406.

(18) (a) Charruault, L.; Michelet, V.; Taras, R.; Gladiali, S.; Genêt, J.-P. Functionalized carbo- and heterocycles via Pt-catalyzed asymmetric alkoxylation of 1,6-enynes. *Chem. Commun.* **2004**, 850–851. (b) Muñoz, M. P.; Adrio, J.; Carretero, J. C.; Echavarren, A. M. Ligand Effects in Gold- and Platinum-Catalyzed Cyclization of Enynes: Chiral Gold Complexes for Enantioselective Alkoxylation. *Organometallics* **2005**, 24, 1293–1300. (c) Chao, C.-H.; Genin, E.; Toullec, P. Y.; Genêt, J.-P.; Michelet, V. Towards asymmetric Au-catalyzed hydroxyl- and alkoxylation of 1,6-enynes. *J. Organomet. Chem.* **2009**, 694, 538–545. (d) Pradal, A.; Chao, C. M.; Vitale, M. R.; Toullec, P. Y.; Michelet, V. Asymmetric Au-catalyzed domino cyclization/nucleophile addition reactions of enynes in the presence of water, methanol and electron-rich aromatic derivatives. *Tetrahedron* **2011**, 67, 4371–4377.

(19) (a) Nieto-Oberhuber, C.; Munoz, M. P.; Lopez, S.; Jiménez-Núñez, E.; Nevado, C.; Herrero-Gomez, E.; Raducan, M.; Echavarren, A. M. Gold(I)-catalyzed cyclization of 1,6-enynes: alkoxylation and *exo/endo* skeletal rearrangements. *Chem. - Eur. J.* **2006**, 12, 1677–1693. (b) Matsumoto, Y.; Selim, K. B.; Nakanishi, H.; Tamada, K.; Yamamoto, Y.; Tomioka, K. Chiral carbene approach to gold-catalyzed asymmetric cyclization of 1,6-enynes. *Tetrahedron Lett.*

**2010**, 51, 404–406. (c) Yamada, K.; Matsumoto, Y.; Selim, K. B.; Yamamoto, Y.; Tomioka, K. Steric tuning of C2-symmetric chiral N-heterocyclic carbene in gold-catalyzed asymmetric cyclization of 1, 6-enynes. *Tetrahedron* **2012**, 68, 4159–4165.

(20) The signs of **4a,d** and **6b** were determined by chiral HPLC and by measuring optical rotatory power according to refs **18a,d**.

(21) Zhang, J.-Q.; Liu, Y.; Wang, X.-W.; Zhang, L. Synthesis of Chiral Bifunctional NHC Ligands and Survey of Their Utilities in Asymmetric Gold Catalysis. *Organometallics* **2019**, 38, 3931–3938.

(22) The signs of **4b,c** and **6a** were determined by measuring optical rotatory power (see the [Supporting Information](#)).

(23) Jia, M.; Bandini, M. Counterion Effects in Homogeneous Gold Catalysis. *ACS Catal.* **2015**, 5, 1638–1652.

(24) Wang, D.; Cai, R.; Sharma, S.; Jirak, J.; Thummanapelli, S. K.; Akhmedov, N. G.; Zhang, H.; Liu, X.; Petersen, J. L.; Shi, X. Silver effect in gold(I) catalysis: an overlooked important factor. *J. Am. Chem. Soc.* **2012**, 134, 9012–9019.

(25) For a review, see: (a) Schmidbaur, H.; Schier, A. Z. Silver-free Gold(I) Catalysts for Organic Transformations. *Z. Naturforsch., B: J. Chem. Sci.* **2011**, 66, 329–350. For recent examples, see: (b) Abadie, M.-A.; Trivelli, X.; Medina, F.; Duhal, N.; Kouach, M.; Linden, B.; Génin, E.; Vandewalle, M.; Capet, F.; Roussel, P.; Del Rosal, I.; Maron, L.; Agbossou-Niedercorn, F.; Michon, C. Gold(I)-Catalysed Asymmetric Hydroamination of Alkenes: A Silver- and Solvent-Dependent Enantiodivergent Reaction. *Chem. - Eur. J.* **2017**, 23, 10777–10788. (c) Weber, D.; Gagné, M. R. Dinuclear Gold-Silver Resting States May Explain Silver Effects in Gold (I)-Catalysis. *Org. Lett.* **2009**, 11, 4962–4965. (d) Homs, A.; Escofet, I.; Echavarren, A. M. On the silver effect and the formation of chloride-bridged digold complexes. *Org. Lett.* **2013**, 15, 5782–5785. (j) Schröder, F.; Tugny, C.; Salanouve, E.; Clavier, H.; Giordano, L.; Moraleda, D.; Gimbert, Y.; Mouriès-Mansuy, V.; Goddard, J.-P.; Fensterbank, L. Secondary Phosphine Oxide–Gold(I) Complexes and Their First Application in Catalysis. *Organometallics* **2014**, 33, 4051–4056. (k) Lu, Z.; Han, J.; Hammond, G. B.; Xu, B. Revisiting the Influence of Silver in Cationic Gold Catalysis: A Practical Guide. *Org. Lett.* **2015**, 17, 4534–4537.

(26) (a) Mézailles, N.; Ricard, L.; Gagosz, F. Phosphines Gold(I) Bis-(trifluoromethanesulfonyl)imide Complexes as New Highly Efficient and Air-Stable Catalysts for the Cycloisomerization of Enynes. *Org. Lett.* **2005**, 7, 4133–4136. (b) Raducan, M.; Rodríguez-Escrich, C.; Cambeiro, X. C.; Escudero-Adán, E. C.; Pericás, M. A.; Echavarren, A. M. A multipurpose gold(I) precatalyst. *Chem. Commun.* **2011**, 47, 4893–4895.

(27) (a) Sak, H.; Mawick, M.; Krause, N. Sustainable Gold Catalysis in Water Using Cyclodextrin-tagged NHC-Gold Complexes. *ChemCatChem* **2019**, 11, 5821–5829. (b) Handa, S.; Lippincott, D. J.; Aue, D. H.; Lipshutz, B. H. Asymmetric Gold-Catalyzed Lactonizations in Water at Room Temperature. *Angew. Chem., Int. Ed.* **2014**, 53, 10658–10662. (c) Minkler, S. R. K.; Lipshutz, B. H.; Krause, N. Gold Catalysis in Miscellar Systems. *Angew. Chem., Int. Ed.* **2011**, 50, 7820–7823.

(28) (a) Nieto-Oberhuber, C.; López, S.; Muñoz, M. P.; Cárdenas, D. J.; Buñuel, E.; Nevado, C.; Echavarren, A. M. Divergent Mechanism for the Skeletal Rearrangement and [2 + 2] Cycloaddition of Enynes Catalyzed by Gold. *Angew. Chem., Int. Ed.* **2005**, 44, 6146–6148. (b) Cabello, N.; Jiménez-Núñez, E.; Buñuel, E.; Cárdenas, D. J.; Echavarren, A. M. On the mechanism of the puzzling “endocyclic” skeletal rearrangement of 1,6-enynes. *Eur. J. Org. Chem.* **2007**, 2007, 4217–4223.

(29) Of note, no reaction of enyne **1** takes place in MeOH with 2 mol % of AgSbF<sub>6</sub>. See also: Nieto-Oberhuber, C.; Muñoz, M. P.; Buñuel, E.; Nevado, C.; Cárdenas, D. J.; Echavarren, A. M. Cationic Gold(I) Complexes: Highly Alkynophilic Catalysts for the *exo*- and *endo*-Cyclization of Enynes. *Angew. Chem., Int. Ed.* **2004**, 43, 2402–2406.

(30) Bursch, M.; Neugebauer, H.; Grimme, S. Structure Optimisation of Large Transition-Metal Complexes with Extended Tight-Binding Methods. *Angew. Chem., Int. Ed.* **2019**, 58, 11078–11087.

- (31) Bannwarth, C.; Ehlert, S.; Grimme, S. GFN2-xTB-An Accurate and Broadly Parametrized Self-Consistent Tight-Binding Quantum Chemical Method with Multipole Electrostatics and Density-Dependent Dispersion Contributions. *J. Chem. Theory Comput.* **2019**, *15*, 1652–1671.
- (32) Bohle, F.; Grimme, S. Efficient structural and energetic screening of fullerene encapsulation in a large supramolecular double decker macrocycle. *J. Serb. Chem. Soc.* **2019**, *84*, 837–844.
- (33) (a) Dorohoi, D. O.; Avadanei, M.; Postolache, M. *Optoelect. Adv. Mater., Rapid Commun.* **2008**, *8*, 511–515. (b) Closca, V.; Ivan, L. M.; Dorohoi, D. O. Intermolecular interactions in binary and ternary solutions. *Spectrochim. Acta, Part A* **2014**, *122*, 670–675. (c) Babusca, D.; Morosanu, C.; Dorohoi, D. O. Spectral study of specific interactions between zwitterionic compounds and protic solvents of two cycloimmonium-carboethoxy-anilido-methylids. *Spectrochim. Acta, Part A* **2017**, *172*, 58–64.
- (34) (a) Licht, E.; Schächter, Y.; Pines, H. Reactions of Binary Mixtures of Primary and Secondary Alcohols Over Reduced Nickel Oxide-Cab-O-Sil Catalysts in the Presence of Hydrogen. *J. Catal.* **1974**, *34*, 338–344. (b) Henkel, S.; Misuraca, M. C.; Troselj, P.; Davidson, J.; Hunter, C. A. Polarisation effects on the solvation properties of alcohols. *Chem. Sci.* **2018**, *9*, 88–89.
- (35) Martin, D.; Lassauque, N.; Donnadieu, B.; Bertrand, G. A Cyclic Diaminocarbene with a Pyramidalized Nitrogen Atom: A stable N-Heterocyclic Carbene with Enhanced Electrophilicity. *Angew. Chem., Int. Ed.* **2012**, *51*, 6172–6175.
- (36) (a) Baskar, B.; Bae, H. J.; Ar, S.E.; Cheong, J. Y.; Rhee, Y. H.; Duschek, A.; Kirsch, S. F. Gold(I)-Catalyzed Divergence in the Reactivity of 3-Silyloxy 1,6-Enynes: Pinacol-Terminated vs Claisen-Terminated Cyclization Cascades. *Org. Lett.* **2008**, *10*, 2605–2607. (b) Alcarazo, M.; Stork, T.; Anoop, A.; Thiel, W.; Fürstner, A. Steering the surprisingly modular pi-acceptor properties of N-heterocyclic carbenes: implications for gold catalysis. *Angew. Chem., Int. Ed.* **2010**, *49*, 2542–2546.
- (37) (a) Mauleón, P.; Zeldin, R. M.; González, A. Z.; Toste, F. D. Ligand-Controlled Access to [4 + 2] and [4 + 3] Cycloadditions in Gold-Catalyzed Reactions of Allene-Dienes. *J. Am. Chem. Soc.* **2009**, *131*, 6348–6349. (b) González, A. Z.; Toste, F. D. Gold(I)-Catalyzed Enantioselective [4 + 2]-Cycloaddition of Allene-dienes. *Org. Lett.* **2010**, *12*, 200–204. (c) Trillo, B.; López, F.; Montserrat, S.; Ujaque, G.; Castedo, L.; Lledós, A.; Mascareñas, J. L. Gold-Catalyzed [4C + 3C] Intramolecular Cycloaddition of Allenedienes: Synthetic and Mechanistic Implication. *Chem. - Eur. J.* **2009**, *15*, 3336–3339. (d) Benitez, D.; Tkatchouk, E.; Gonzalez, A. Z.; Goddard, W. A., III; Toste, F. D. On the Impact of Steric and Electronic Properties of Ligands on Gold(I)-Catalyzed Cycloaddition Reactions. *Org. Lett.* **2009**, *11*, 4798–4801. (e) Alonso, I.; Trillo, B.; López, F.; Montserrat, S.; Ujaque, G.; Castedo, L.; Lledós, A.; Mascareñas, J. L. Gold-Catalyzed [4C+2C] Cycloadditions of Allenedienes, including an Enantioselective Version with New Phosphoramidite-Based Catalyst: Mechanistic Aspects of the Divergence between [4C + 3C] and [4C+2C] Pathways. *J. Am. Chem. Soc.* **2009**, *131*, 13020–13030.
- (38) (a) Liske, A.; Verlinden, K.; Buhl, H.; Schaper, K.; Ganter, C. Determining the  $\pi$ -Acceptor Properties of N-Heterocyclic Carbenes by Measuring the  $^{77}\text{Se}$  NMR Chemical Shifts of Their Selenium. *Organometallics* **2013**, *32*, 5269–5272. (b) Vummaleti, S. V. C.; Nelson, D. J.; Poater, A.; Gomez-Suarez, A.; Cordes, D. B.; Slawin, A. M. Z.; Nolan, S. P.; Cavallo, L. What can NMR spectroscopy of selenoureas and phosphinidenes teach us about the  $\pi$ -accepting abilities of N-heterocyclic carbenes? *Chem. Sci.* **2015**, *6*, 1895–1904. (c) Verlinden, K.; Buhl, H.; Franck, W.; Ganter, C. Determining the Ligand Properties of N-Heterocyclic Carbenes from  $^{77}\text{Se}$  NMR Parameters. *Eur. J. Inorg. Chem.* **2015**, *2015*, 2416–2425.
- (39) Nelson, A.; Collabo, D. J.; Manzini, S.; Meiries, S.; Slawin, A. M. Z.; Cordes, D. B.; Nolan, S. P. Methoxy-Functionalized N-Heterocyclic Carbenes. *Organometallics* **2014**, *33*, 2048–2058.